Computers and Structures 167 (2016) 24–36

Contents lists available at ScienceDirect

Computers and Structures

journal homepage: www.elsevier.com/locate/compstruc

Concurrent design and process optimization of forging

Murat Ozturk, Sinem Kocaoglan, Fazil O. Sonmez *

Department of Mechanical Engineering, Bogazici University, Istanbul 34342, Turkey

ARTICLE INFO

Article history:
Received 7 September 2015
Accepted 28 January 2016

Keywords:
Concurrent engineering
Metal
Cold forging
Optimization
Global optimum
FEM

ABSTRACT

In this study, a concurrent design optimization methodology is proposed to minimize the cost of a cold-forged part using both product and process design parameters as optimization variables. The objective function combines the material, manufacturing, and post manufacturing costs of the product. The part to be optimized is a simply supported I-beam under a centric load. Various constraints are imposed related to the performance of the product in use and the effectiveness of manufacturing. Nelder–Mead is used as search algorithm and analyses are conducted using commercial finite element software, ANSYS. Results show considerable improvement in the cost.

1. Introduction

Various manufacturing methods can be used to produce mechanical parts. A suitable method is chosen based on the geometry of the part, the required quality, the quantity to be produced, and the manufacturing cost. In this study, forging is considered, which is one of the widely used manufacturing methods for metals. If the forming process occurs below the recrystallization temperature of the metal, the process is called 'cold forging.' This has certain advantages such as high dimensional accuracy, superior mechanical properties and microstructure, better surface finish, and no oxidation. Furthermore, forging to net or near-net shape dimensions reduces material as well as post processing cost. However, because of relatively high tooling and equipment costs, the process is feasible only if the part is to be produced in large quantities [1].

In the traditional approach, manufacturing procedure is decided based on experience. In most cases, values for processing parameters selected based on experience and intuition do not give satisfactory results. Hence, they are modified via a trial-and-error-correction method. For manufacturing processes requiring high tooling costs, these trial-and-error efforts drastically decrease the efficiency of the product development phase. Besides, the resulting processing conditions would be less than the optimum. The traditional approach has become obsolete with the developments in the computational technology. Numerical methods like FEM allow prediction of the effects of process parameters on the end product by simulating the manufacturing process. This reduces trial-and-error efforts dramatically. On the other hand, FEM as an analysis tool only provides outputs for a given process; it cannot appraise these outputs and suggest a better processing scheme. Integration of simulation models with optimization algorithms helps to determine the optimum processing conditions. The forging process has a number of parameters that are under the control of the process designer, which can be used to optimize the process. By optimizing the controllable processing parameters, one can improve the product quality and manufacturing efficiency, and decrease costs considerably. In a process optimization study, according to the desired optimization aim, a suitable objective function is constructed. Choosing appropriate objective and constraint functions, optimization variables, and search algorithm has utmost importance on the effectiveness of the optimization. In the literature, different approaches were adopted in this respect.

In the previous studies of forging process optimization, the researchers considered forging of blocks by upsetting [2–15], H-shaped axisymmetric parts [5,6,16–25], I-beams [26,27], aerofoil blades [3,28–32], hollow cylinders [15], axisymmetric parts like disks or cups [2,8,13,25,27,32–43,44], other 2D parts [43,45], steering links [46], wheels [31,45], hubs [47,48], spindles [49], gears [49], and other 3D parts [10,50]. In some of these studies, forging process was simulated as hot [2,4–6,13,16,17,21–23,25–30,32,34,35,37,39,43,44–46,48–50], in others [11,14,17,20,27,32,33,36,38,40–42,47] as cold.

In an optimization procedure, depending on the quality and cost requirements on the part, a suitable objective function is chosen. In

* Corresponding author. Tel.: +90 212 359 7196; fax: +90 212 287 2456.
E-mail address: sonmezfa@boun.edu.tr (F.O. Sonmez).

http://dx.doi.org/10.1016/j.compstruc.2016.01.016
0045-7949/

the previous studies, the goal was to minimize the deformation energy [19,20,49], the difference between the desired shape and the final realized forged shape [2,3,7–11,13,23,25,26,28–30,32], cost [52], excess material or flash, which is the portion of the workpiece bulging out of the die, in order to obtain net shape [35,47], unfilled area of die [27], damage index of the workpiece [38,40], variation in hardness distribution [33], variation in grain size [21], variation in the temperature [34], variation in effective strain [22,24,41–43,46,48], maximum strain rate to avoid folding defect [45,49], die wear [18]. In another study [36], die fatigue life was maximized. Besides, multi-objective optimization problems were considered where the objective was to minimize the forging energy and the difference between the realized and prescribed final forged shape [4–6,12,14–16,44], unfilled area of die and forging energy [42], unfilled area of die and flash area [17,31], unfilled area of die, forging energy, and strain variation [39] total strain energy, strain variation, and forging force [37], material use, total strain energy, and strain variation [43]. In some cold forging operations, deformation becomes so extensive that forging operations are conducted in sub-steps followed by annealing. In order to obtain the desired shape or avoid forging defects, more than one forging operation may be needed even in hot forging. Hence, in some studies [4–6,7,8,17,18,23–26,34,38,40,44,49], forming stages were optimized.

In forging process optimization studies, optimization variables are chosen among the processing parameters that have an effect on the objective function. Parameters defining preform-die shape or final-die shape [2–6,7,8,16–18,20,23–26,28–32,36,38–40,43–45,49], fillet radii of the die [20,33,37], preform shape [5,6,9,11–15,31,35,41,43,50,46,48], preform dimensions [17,19,21,27,33,37–40,47,49] number of forming operations [40], thickness of the flash [20], initial temperature [4,14,16,22,34,30], ram velocity [12,21,22,34,39], pressure or force applied by the tools [42,50], stroke [17,22,30], were selected as optimization variables in the process optimization problems considered in the previous studies.

In a process optimization procedure, while improving the objective function by modifying the optimization variables, constraints are imposed on these variables to avoid underfilling of the die cavity [5,8,16,19,21,22,35,37,41,42,46–48], folding or wrinkling [2,15,23,35,37,50], the difference between the produced shape and the target shape [3,8–10], shape errors [10], excessive flash [21]. Constraints are also applied to limit the maximum strain [40], the variation in strain [19], effective strain rate [34], maximum temperature [4,14,16], maximum pressure on the die [40], and forging load [22].

Effectiveness of an optimization procedure depends on the search algorithm. Some researchers used stochastic global search algorithms like genetic algorithms [2,4,12,14–17,38,40]. Some other researchers used gradient [5,6,7–11,13,18,21,23–26,28,44,45] or non-gradient [29,31,33,34] based local search algorithms. In many of the previous studies, a meta (or surrogate) model is constructed representing the objective and constraint functions using response surface method [3,19,22,30,32,41,42,46,48,49], artificial neural networks [27,39], multivariate polynomial interpolation [37], or Kriging [37,49], then optimization is conducted using the model via a local search method. If few parameters are used as optimization variables, a parametric study [20,35,36,43,47,50] may be conducted to improve the forging process.

In most applications, the manufacturing efficiency, manufacturability, cost, and quality of the resulting product depend on both processing and design parameters. For this reason, integrating product design and manufacturing design phases, which is called concurrent design approach, enables consideration of interacting effects of these parameters. Accordingly, designing forged products includes not only the optimization of the part geometry and material but also the selection of appropriate manufacturing process conditions so that desired properties can be obtained (strength, tolerances, residual stresses, grain structure, surface properties, etc.) with minimum cost. Through the use of a concurrent design procedure with an optimization algorithm, both manufacturing process and part performance can be optimized. A concurrent design optimization scheme includes both design and processing parameters as optimization variables and also design and manufacturing constraints. Some concurrent design optimization procedures were previously developed by several researchers [51–54] for some manufacturing processes. Chang and Bryant [53] minimized the cost of aircraft torque tubes, piston and cylinder components and the tube weight by using the part thicknesses as optimization variables. The design and the processing were optimized concurrently to minimize the volume while maintaining its strength. Al-Ansary and Deiab [54] minimized the total machining cost of mechanical assemblies including the cost of all individual machining operations by taking product design dimensional tolerances and machining tolerances as optimization variables. They considered two mechanical systems, piston-cylinder assembly and rotor assembly, and optimized the tolerances of their individual parts. Janakiraman and Saravanan [52] minimized the total manufacturing cost and the deviation from the targeted performance. Three cost components, operation cost, tool cost, and tool replacement cost, were included in the objective function. Number of rough turning passes, cutting speed, feed and depth of cut in each step were taken as optimization variables; upper and lower limits were set on machining parameters, cutting force, power, and surface roughness. Chen and Simon [55] optimized product performance and welding process. Height of the beam, its thickness, depth and length of the weld were selected as optimization variables. Constraints were imposed on these parameters to avoid large deflection and static and buckling failure. There is only one study on forging process optimization using a concurrent approach [51]; however it is rather on the development of a support software module aimed at assisting manufacturing design decisions. This system combined theoretical and empirical knowledge about a variety of aspects of product design and manufacturing, and thus, it provided guidance for engineers to decide on some factors like material type, lubricant, and machine type. In that respect, the present study can be considered to be the first study on the concurrent optimization of forging processes. Besides, in comparison to the forging optimization studies that considered a part with a similar geometry like reference [20], a larger number of parameters are considered as optimization variables and also a larger number of constraints. Therefore, the present study is more comprehensive in regard to processing optimization.

2. Problem statement

The aim of this study is to develop a concurrent design optimization methodology for the combined optimization of product design and processing design phases of a forged part. The methodology is applied to a simply-supported beam with an I-cross section subjected to a centric load as the worst loading condition during its use as shown in Fig. 1. I-beams are generally used in the industry due to their good load carrying capacity under bending.

Manufacturing of an I-beam can be achieved by forging, extrusion, or roll forming. The choice between these methods is made based on the feasibility, the manufacturing cost, the target mechanical properties, and the dimensions of the beam. The part considered in this study is a short beam with dimensions $400 \times 45 \times 35$ mm with large web and flange thickness (about 10 mm); forging can then be considered to be a suitable processing method. Accordingly, the manufacturing method is chosen to be

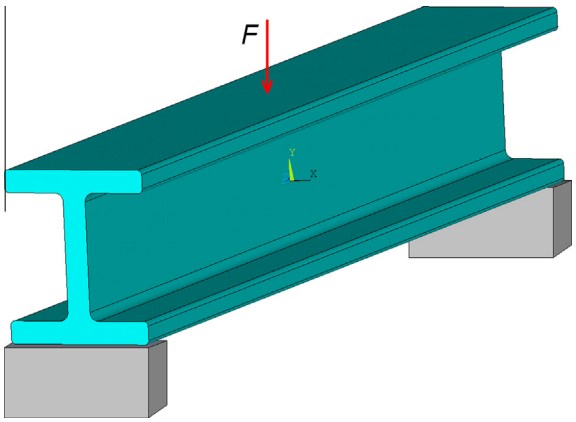

Fig. 1. A schema of simply supported I-beam under centric load.

cold forging followed by shearing and machining operations. As illustrated in Fig. 2, first a rectangular bar is forged into an I-beam and this operation is followed by the shearing of the flashes. The cut regions are then machined.

The objective is to find the globally optimal values of the design and processing variables to minimize the total cost including the material cost and the manufacturing cost. The optimization is subject to both behavioral and manufacturing constraints. The behavioral constraints include failure conditions due to static yielding and local buckling during the use of the beam. Satisfaction of these constraints ensures safe use of the part. The manufacturing constraints include die filling, the maximum allowable pressure on the die, and limited flash out of the die. In this way, the billet fills up the die, no damage is done to the dies during forging, and the length of the flashes, i.e. material waste, is minimized. Both manufacturing and design parameters are chosen as optimization variables. Design variables are the dimensions of the I-beam; manufacturing variables are the fillet radii, thickness of the flash, and the preform dimensions.

3. Optimization methodology

The purpose of optimization is to find the best possible configuration among many potentially viable configurations for a given use according to a chosen performance criterion. A typical design optimization problem is solved through the following stages: Formulation of objective function to be minimized; selection of design variables affecting the value of the objective function and constraint functions; setting the constraints; defining penalty functions, weight coefficients; selection of search algorithm.

3.1. Design variables

Effectiveness of the optimization procedure depends on the proper choice of optimization variables. All the parameters having considerable effect on the objective function or the constraint functions should be chosen as optimization variables for effective optimization. On the other hand, the parameters having insignificant effect should be taken as constant to avoid unnecessary computational burden.

Fig. 3 shows the cross-section of the I-beam and the geometric parameters defining the section. Because I-beams are doubly symmetric, one of the representative quarters is considered in the analysis of the forging process as depicted in Figs. 3 and 4. Forging is achieved by forcing the upper die to move a certain distance, s. The stroke, s, depends on the height of the preform, $2H$, and the thickness of the web, t_w. The parameters chosen as optimization variables include the design variables, which are the thickness of the flange, t_f, thickness of the web, t_w, width, b, height, h_f, fillet radii, r_1, r_2, r_3, and r_4, half of the preform dimensions, H and L, and half burr thickness, t_b. Among these, there are design parameters as well as processing parameters. The design parameters are the dimensions of the cross-section, t_f, t_w, h_f, b; these mainly affect the performance of the part. The processing parameters are the preform dimensions, H and L, the fillet radii, r_i, and the burr thickness, t_b; these mainly influence the effectiveness of manufacturing. Length of the preform, L, is not directly taken as a variable; instead the volume of the die cavity, V_d, is calculated and L is expressed as

$$L = V_d/H + \ell \tag{1}$$

Here ℓ is taken as optimization variable. The draft angles of the flange, α_1 and α_2, are taken as constant and equal to 3° as in the study of Khoury et al. [20]. Table 1 gives the relations between the parameters and also the values of the parameters taken as constant.

3.2. Formulation of the objective function

Solution of an optimization problem first requires definition of an objective function that serves as a criterion for the effectiveness of a design. In this study, the goal is to minimize the overall cost

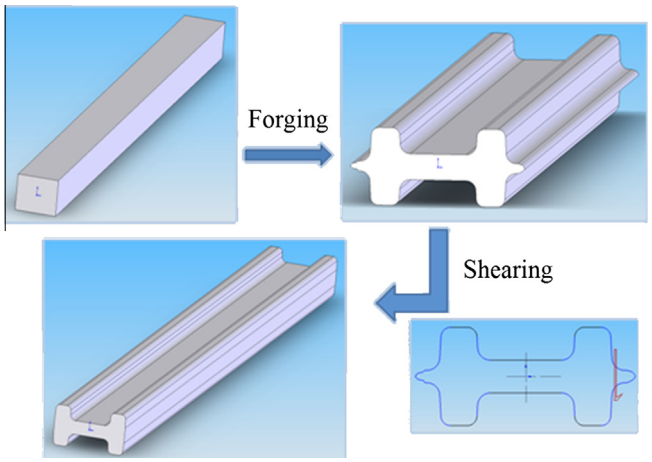

Fig. 2. Manufacturing phases of the I-beam [56,57].

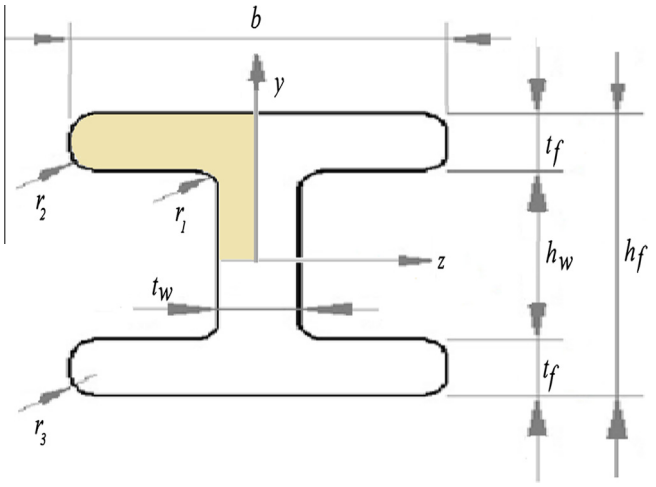

Fig. 3. Cross-sectional shape of the I-beam.

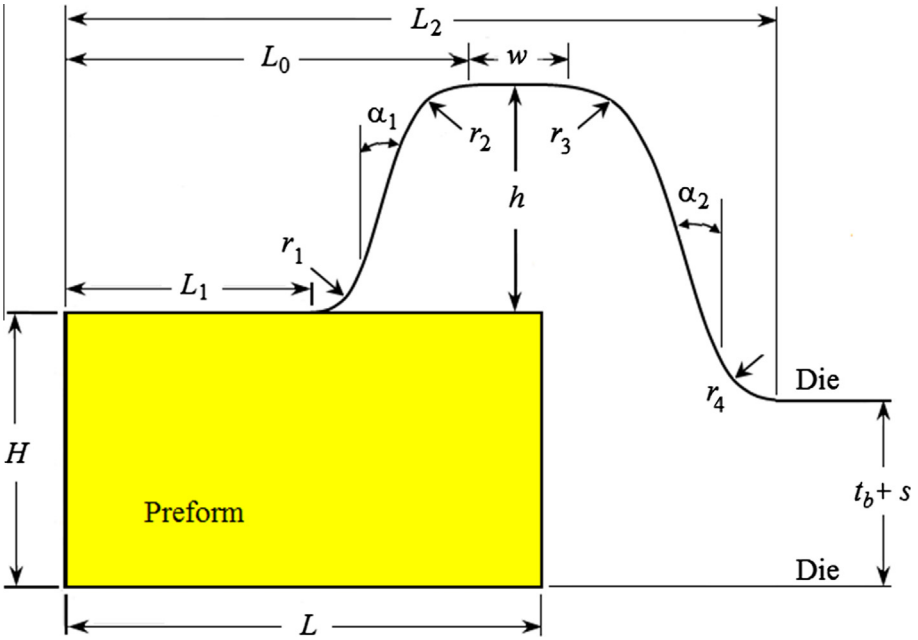

Fig. 4. Cross-sectional dimensions of a quarter of the I-beam processed by forging.

Table 1
The geometric parameters.

Width	$b = 2(H + h - s)$
Height	$h_f = 2(L_0 + w + r_3)$
Flange Thickness	$t_f = w + r_2 + r_3$
Web height	$h_w = h_f - 2t_f$
Half of web height	$L_1 = L_0 - r_1 - r_2 - (h - r_1 - r_2)\tan\alpha_1$
Stroke	$s = H - t_w/2$
Beam length	$L_b = 400$ mm
Draft angles	$\alpha_1, \alpha_2 = 3°$

without violating the constraints. Accordingly, the objective function to be minimized is expressed as

$$f = c_{mat} + w_f c_f + w_s c_s + c_{mch} + \sum_{i=1}^{n} c_i P_i \tag{2}$$

where c_{mat} is the material cost, c_f is the cost of the forging process, c_s is the cost of the shearing operation, c_{mch} is the machining cost, P_i are the penalties, c_i are the penalty coefficients, and n is the total number of the constraints. The first four terms have the same unit, which is chosen as dollar. The last term takes nonzero value only in case of constraint violations.

It should be noted that f is not equal to the total cost of the product; the costs that are independent of the optimization variables are not included in the objective function. Constant terms added to the objective function do not influence the optimization process, in which the value of the objective function is minimized by varying the values of the optimization variables. Labor, die, and machinery costs are usually considered as such and they are not taken into account in process optimization studies. However, the optimization variables may have some effect, even if small, on these costs. If a larger energy is spent in forming the part or cutting the flash, increased wear and depreciation may occur in the machinery or operation time may become longer. However, finding an explicit and general relation is not possible; this depends on the type and quality of the machinery and the tools. In this study, in order to account for these effects, w_f and w_s factors are introduced. A value of 20 is taken for both factors. Because, these effects can directly be taken into account for the machining cost, c_{mch}, a factor is not introduced for this term.

3.2.1. Material cost, c_{mat}

The material cost in terms of dollars can be expressed as

$$c_{mat} = p_{mat}\rho V \tag{3}$$

where p_{mat} is the unit price of the material in terms of dollars per kilogram, ρ is the density of the material in terms of kg/m^3, V is the volume of material used to produce the part. Considering that the volume of the material does not change with plastic deformation, V can be expressed in terms of the preform dimensions as

$$V = 2H \cdot 2L \cdot L_b \tag{4}$$

where L_b is the length of the I-beam (see Table 1). The factor "2" appears because only one fourth of the preform is analyzed (see Fig. 4).

3.2.2. Forging cost, c_f

The cost of the forging operation is related to the energy spent to deform the workpiece. This energy is assumed to be proportional to the total strain energy of deformation of the final part, U_f, which can be formulated as

$$U_f = 4L_b \int_0^t \iiint \sigma_{ij}\dot{\varepsilon}_{ij} dV dt \tag{5}$$

where σ_{ij} are the components of the stress tensor and $\dot{\varepsilon}_{ij}$ are the total (elastic and plastic) strain rates (there is sum on i and j). The expression in Eq. (5) is not calculated analytically. The values of strain energy in the finite elements are stored in the element tables of ANSYS and they are used to calculate the total strain energy. U_f is four times the strain energy calculated using finite elements, because one fourth of the preform is analyzed. Considering that a 2D plane strain structural analysis is carried out; the FE software yields strain energy per unit thickness, which should be multiplied by the length of the beam, L_b, to obtain the total strain energy.

The cost of forging in terms of dollars as the cost of electricity spent during forging is expressed as

$$c_f = p_e U_f / \eta_f \tag{6}$$

where p_e is the local electricity price for industry in terms of dollars/Joule, η_f is the efficiency with which electricity is converted to deformation energy, which is taken as 0.3.

3.2.3. Shearing cost, c_s

As a post manufacturing cost, there is cost of energy required to cut the flashes at the sides of the forged part. The shearing energy is calculated analytically using the following formula [58]:

$$U_s = c_{11}c_{22}S_{ut}(2t_b)^2L_b \tag{7}$$

where c_{11} is a constant equal to 0.85 for ductile materials, c_{22} is a constant equal to 0.5 for soft materials, $2t_b$ is the burr thickness, and S_{ut} is the tensile strength of the material. The cost of the shearing operation is expressed similar to the cost of forging as

$$c_s = 2p_eU_s/\eta_s \tag{8}$$

where η_s is the efficiency of the shearing operation, which is also taken as 0.3. The equation includes the factor '2' because there is one flash at each side.

3.2.4. Machining cost, c_{mch}

The whole top and bottom surfaces of the beam are machined. After the flash is removed, the cut region will have a rougher surface and thus there will be additional machining cost. The total machining cost depends on the width of the beam, b, and the burr thickness, $2t_b$. It is expressed as

$$c_{mch} = 2[p_{fm}(2t_bL_b) + p_m(b - 2t_b)L_b] \tag{9}$$

where p_{fm} is the cost of machining per unit area of the cut region, $(2t_bL_b)$ is the area of the cut region, p_m is the cost of machining per unit area of the uncut forged surface, $(b - 2t_b)L_b$ is the area of the uncut region on the top or bottom surface. The equation includes the factor '2' because there is a flash on both the top and bottom surfaces.

3.3. Constraints and penalty functions

In typical product design or processing design problems, a number of constraints need to be imposed on the variables in order to obtain acceptable solutions. The constraints define the feasible domains for the optimization variables. Selection of the constraint limits may be based on the process requirements like filling of the die cavity, or product requirements like strength and ergonomic considerations. If the feasible domain is arbitrarily restricted, better solutions may be missed. If it is unnecessarily large, search for the optimum design may require increased computational effort.

In this study, constraints are imposed on the optimization variables based on the design and process requirements, and possible numerical problems in the FE analysis. Behavioral constraints are used to avoid failure of the finished product during service as a design requirement. For the present problem, local buckling failure and static failure in the form of yielding are considered as behavioral constraints. The manufacturing constraints considered in this study are filling of the die cavity, failure of the mold, and limited flash. There are also side constraints like limits on the cross-sectional dimensions of the beam due to spacing requirements, or limits beyond which no feasible or optimum design is expected like very small or very large fillet radii.

There are mainly two ways to incorporate constraints: One is to introduce penalty functions, thus transform the constrained optimization problem into an unconstrained one and then solve the problem using a search algorithm suitable for unconstrained problems. The second approach is to use a search algorithm developed particularly for constrained problems like feasible directions method. Considering the high number of variables and the constraints, and the complexity of the feasible region in the problem considered in this study, the first approach is adopted. If the constraints are violated, a penalty is added to the objective function. Because the search algorithm tries to find designs with lower objective function values, penalties force the optimization algorithm to search the optimum design within the feasible domain, where no constraint is violated.

There are a number of constraint types. First of all, upper and lower limits, x_u and x_l, may be set for the optimization variables. These inequality constraints can be expressed as

$$x_l < x < x_u \tag{10}$$

If the search algorithm assigns a value to this variable outside its feasible range, a penalty is added to the objective function. If the lower bound is exceeded, the penalty function is defined as

$$P = c\left\langle \frac{x_l - x}{x_u - x_l} \right\rangle \tag{11}$$

and if the upper bound is exceeded, it is defined as

$$P = c\left\langle \frac{x - x_u}{x_u - x_l} \right\rangle \tag{12}$$

Because the type of these penalty functions is external, they become active only if their corresponding constraint is violated. Otherwise, they are equal to zero. This condition is controlled by the operator "<>". If the value of the term inside this operator is positive, it yields the same value; otherwise it yields zero.

Although, burr (or flash) length, L_f, is not an optimization variable, upper and lower limits are set to avoid underfilling due to a negative value of L_f or excessive material waste due to a large flash. After the process simulation is completed in each iteration, the flash length is obtained via FE post processing. The penalty value is then calculated in the same manner as indicated in Eqs. (11) and (12).

In order to avoid underfilling and ensure complete die fill, the contact condition at each contact element in the interface between the die and the workpiece is checked. If the software predicts that these boundary elements in the interface are open or if the number of elements that are open but at near contact exceeds 6% of the elements in the interface, then a penalty value is calculated in the following manner:

$$P = c_1n_o + c_2\langle n_{po}\% - n_{all}\% \rangle \tag{13}$$

where n_o is the number of completely open elements at the interface, n_{po}% is the percentage of interface elements that are open but at near contact; n_{all}% is taken as 6%; c_1 and c_2 are penalty coefficients, which are taken as 50 and 3, respectively.

Another constraint used in the optimization procedure is the maximum allowable contact pressure on the die, which may cause permanent deformation or fracture in the die. If the maximum contact pressure on the contact elements at the interface between the die and the workpiece, p_{max}, exceeds the allowable compressive stress of the mold material, σ_{all}, a penalty is added to the objective function as

$$P = c\left\langle \frac{p_{max} - \sigma_{all}}{\sigma_{all}} \right\rangle \tag{14}$$

Steel punches are limited to approximately 1200 MPa and cobalt-bonded WC punches are limited to approximately 3300 MPa [59]. In this study, the allowable contact pressure on the die is taken as 1200 MPa. In order to be on the safe side, the upper limit on the maximum contact pressure, σ_{all}, is chosen as 10% lower than this value.

If the maximum equivalent stress, σ_{max}, developed in the part due to the loads applied during its use exceeds the yield strength of the material, S_y, static failure occurs. In such a case, a penalty is calculated using an equation similar to Eq. (14). A similar penalty function is also defined for buckling failure.

The values of the penalty coefficients, c, in Eqs. (11)–(14), used in the optimization procedure significantly affect the effectiveness of the optimization process. If the feasible domain is a convex region, large values are chosen to force the algorithm to search only within the feasible domain. On the other hand, if the feasible domain is nonconvex and complex, besides it consists of patches separated by infeasible region as in the present problem, low values of c allow a more effective search of the solution domain; but the values of c should be large enough to prevent convergence within the infeasible domain. In this study, most of the penalty coefficients are taken to be 10.0. Two times of this value is chosen for the penalty coefficients of the constraints concerning the upper limit on height, h_f, and the static failure constraints, because in some runs, convergence occurred while these constraints were still not satisfied. A large value is also chosen for c_1 coefficient in Eq. (13), because the die-fill constraint proved to be critical.

During the optimization process, the value of the objective function is recalculated whenever the values of the optimization variables are changed by the search algorithm. In order to simulate the large deformation during forging, a non-linear FE analysis is performed. One of the problems that may arise is the failure of analysis. The search algorithm may generate a set of variables such that, for some reason, FE analysis fails, e.g. the geometry may not be constructed due to a negative value assigned to radius of curvature, or analysis may not be completed due to a sharp corner or excessive deformation. If FE analysis fails, the objective function cannot be calculated. In such a case, a large penalty value, which is 200, is assigned to the objective function.

In cold forged parts, large variation in strain is not desired. Under impact loading, premature fracture may occur in highly worked hardened regions. Fatigue resistance may also be adversely affected. However, because the I-beam considered in this study is subjected to quasi-static loading during its use, no constraint is imposed on the effective strain variation.

Because closed die forging is employed rather than open-die forging, the forged part is assumed to be dimensional accurate for the particular application; besides no significant elastic spring back is expected as in sheet-metal forming. Accordingly, no constraint is needed to ensure dimensional accuracy of the forged part.

3.4. Optimization procedure

The objective of the optimization problem considered in this study is to minimize the cost of manufacturing and material at the same time satisfying the design and processing constraints. One difficulty of the present problem is the search for the optimum design with a large number of variables. If the problem were to make an improvement on a currently used design by optimization, this could be achieved via a local optimization in the vicinity of the current design by allowing small changes in the values of the variables; then a high number of variables would not be a problem. However, in the present problem the objective is to find the globally optimal design or a near global optimum design. In order to achieve this, first the range of values that can be assigned to the optimization variables should be large, i.e. the solution domain should be large so that the best possible designs would not be left outside the domain within which search is conducted. Secondly, either a global search algorithm should be used or a local search algorithm should repeatedly be employed starting from randomly chosen initial points. Either way, global search is computationally expensive. The second difficulty is that the optimization variables include both design parameters and manufacturing parameters. A manufacturing process can only be optimum for a particular design. In an optimization procedure where the design is continuously varied, processing cannot be effectively optimized at the same time. For these reasons, a multilevel optimization approach is adopted in this study. In the first level, using only the design variables, the part design is optimized within a large solution domain considering only the design constraints. In the second level, all of the design parameters and the processing parameters are used as optimization variables to find the optimum concurrent design; but the range of values for the design variables is taken to be small so that processing can effectively be optimized. In this way, a local search is performed around the optimal design obtained in the first level, while the processing is being optimized.

3.4.1. First level optimization

In the first stage, the product design is optimized by minimizing the material cost. Because, the preform dimensions are determined in the second level, only the material used in the part, not the material used in the forging process, is minimized. Besides, manufacturing cost, which is calculated in the second level, is not included. In the first level optimization, the width, b, and the height, h_f, of the cross section, the thicknesses of the web, t_w, and the flange, t_f, (see Fig. 3) are used as optimization variables. The objective function is expressed as

$$f_1 = p_{mat}\rho V_p + \sum_{i=1}^{m} c_i P_i \tag{15}$$

where p_{mat} is the unit price of the material ($/kg), ρ is the density, V_p is the volume of the part, which is calculated as AL_b. In evaluating the cross-sectional area, A, the fillet radii, r_i, are also taken into account. Fillet radii, which are optimized in the second level, are taken as 3 mm in the first level.

The behavioral constraints, which are static failure and buckling failure, as well as the side constraints are applied in the first level. The side constraints are the chosen upper and lower limits on the optimization variables. The limits are given in Table 2. The upper limits on h_f and b are chosen based on the spacing requirements. The other limits are chosen such that beyond them no feasible or optimum solution is expected; they just serve to limit the search domain in order to avoid unnecessary calculations.

3.4.2. Second level optimization

In the second level, the total cost of the I-beam including the material, forging, shearing, and machining costs is minimized. Accordingly, the expression in Eq. (2) is used as the objective function. All of the design parameters (the width, b, and the height, h_f, of the cross section, the thickness of the flange, t_f, and the web, t_w), and all of the processing parameters (fillet radii, r_1, r_2, r_3, and r_4, half of the preform dimensions, H and L, and half burr thickness, t_b; see Fig. 4) are considered as optimization variables in the second level. As mentioned before, ℓ not L is taken as optimization variable, which is defined in Eq. (1). All of the aforementioned constraints are imposed in the second level including side constraints, processing constraints, and behavioral constraints, i.e. static failure and buckling failure.

Table 3 shows the upper and lower limits on the constrained parameters. L_f and t_b are the length and thickness of the burr (or flash), respectively. Flash length, L_f, is not an optimization variable. After FE simulation is conducted, its value is obtained via the post processing module. Its lower limit is zero. A negative value indicates that grooves will take form at the top and bottom of the beam, that means complete die fill requirement will not be satisfied. On the other hand, the larger this value, the more materials

Table 2
The upper and lower limits (in mm) on the variables used in the first level.

$40 \leqslant h_f \leqslant 45$
$30 \leqslant b \leqslant 35$
$0.5 \leqslant t_f \leqslant 20$
$0.5 \leqslant t_w \leqslant 20$

Table 3
The upper and lower limits (in mm) on the parameters in the second level.

$1 \leqslant r_1 \leqslant 10$	$-0.9 \leqslant \ell \leqslant 1$
$1 \leqslant r_2 \leqslant 7$	$0.2 \leqslant t_b \leqslant 8$
$1 \leqslant r_3 \leqslant 8$	$16 \leqslant H \leqslant 28$
$1 \leqslant r_4 \leqslant 10$	$0 \leqslant L_f \leqslant 2$

waste is produced, which is also not desired. The limits for the product design variables are the same as those given in Table 2.

The ranges for allowable values for the parameters are selected as wide as possible. Beyond these limits, either difficulties are observed in generating the shape and obtaining FE solution, or optimum configurations are not expected. In the optimization runs, none of the processing variables converged to a value close to its constraint limit.

3.5. Search algorithm

As mentioned before, FE analysis of the forging process fails for some configurations generated by the search algorithm. Because the objective function cannot be calculated in these cases, a large penalty value is assigned to the objective function. If FE simulation fails, it is then not possible to evaluate derivatives of the objective function. Therefore, first or second order search algorithms cannot be used in the solution of the present problem, even though they are more efficient. Considering that zero order methods do not require derivatives of the objective function, they can be applied to the present problem. Among them are stochastic and deterministic methods. The advantage of stochastic methods like simulated annealing and genetic algorithms is that they may start from any set of values for the optimization variables irrespective of whether they are satisfying the constraints, or not and find the global minimum. However, they are more difficult to apply and computationally expensive. Zero-order deterministic methods like Nelder–Mead and Powel's method are much easier to apply; only starting points need to be specified; but they may easily miss the global optimum. In order to find the globally optimal configuration, a deterministic local search algorithm should be employed many times starting from different points within the feasible region. Then, the lowest value is chosen as the global minimum or near global minimum of the objective function. For a complex structural optimization problem, it was shown in reference [60] that a global search algorithm is computationally more effective than a local search algorithm repeatedly used starting from random points within the feasible domain. Nevertheless, a local algorithm is preferred in this study considering that many initial runs are needed to determine suitable values for penalty coefficients and the extent of the solution domain. Because it is a robust zero-order search algorithm, Nelder–Mead [61] is chosen as the search algorithm to find the optimum values of the design and processing variables.

In computationally expensive optimization problems, use of response surface method (RSM) may significantly reduce computational time. In the standard application of RSM, the objective function is represented by a quadratic function. Considering that a complex objective function approximates a quadratic function only around its extremal points [62], RSM is not a proper method for the present problem. In the present study, because the globally optimal configuration is sought, the ranges of values that can be assigned to the optimization variables are taken to be large; that means the solution domain within which the algorithm searches the optimum configuration is large. A highly nonlinear objective function cannot be accurately represented by a quadratic function within a large domain. However, a hybrid approach is viable; that means first a global search algorithm can be used to find the regions potentially containing the global optimum or a near global optimum. Within a smaller solution domain, the objective function can be fit to a quadratic function using RSM. Then using a local search algorithm, the optimal configuration can be located. However, because of the aforementioned reasons, use of a global search algorithm is not preferred as the first choice.

In the first level, while optimizing the design of the I-beam, analytical formulas are used for the objective and constraint functions, which can be evaluated in a fraction of a second; therefore efficiency of the search algorithm is not an issue. For this reason, even though more efficient higher order search algorithms can be utilized in the first level, Nelder–Mead is used as in the second level. In the first level, the optimization code initially selects random values for the four optimization variables within their feasible range given in Table 2. Because Nelder–Mead requires $k + 1$ initial configurations to start the search for the optimum configuration, k being the number of design variables, five configurations are randomly generated. The material cost and penalty values are calculated to determine their objective function values. If a local search algorithm is used, normally initial configuration is chosen within the feasible domain, otherwise convergence may occur on a local minimum outside the feasible domain. In the present study however, as long as the geometry of the beam can be constructed with the randomly chosen values for the dimensions, satisfaction of the design constraints is not required for the initial configurations. After initiation, new configurations are generated in each iteration and the five current configurations are updated according to the decision criteria of Nelder–Mead algorithm. Iterations are continued until the difference between the objective function values of the current configurations can be considered to be very small, which is less than 0.005$. Convergence is achieved in the first level at most in 150 iterations. Because Nelder–Mead is a local search algorithm, the optimum configuration found after a search is completed cannot be considered as the globally optimal configuration. For this reason, the search process should be repeated many times starting from randomly generated configurations such that the best configuration is found a number of times. In order to check the validity of this approach, the optimization process is repeated 100 times. The best result is found five times; accordingly it is considered as the global optimum. If the difference between the objective function value of a configuration and that of the global optimum is less than 1%, that configuration is considered as a near global optimum. 16 near global optimum configurations are found in 100 searches. One may conclude that if the optimization process is repeated about 20 times, there is a very high likelihood of locating the global or a near global optimum in the first level.

In the second level, both the product design and the processing design are optimized using the four design and seven processing variables. This means that the optimal design found in the first level is allowed to vary in the second level; but it is varied within the neighborhood of the optimal design. This is achieved by randomly choosing initial designs not within the limits given in Table 2, but within narrow the limits given by

$$\begin{aligned} 0.94h_{f.opt} &\leqslant h_{f.ini} \leqslant 1.06h_{f.opt} \\ 0.94b_{opt} &\leqslant b_{ini} \leqslant 1.06b_{opt} \\ 0.94t_{f.opt} &\leqslant t_{f.ini} \leqslant 1.06t_{f.opt} \\ 0.94t_{w.opt} &\leqslant t_{w.ini} \leqslant 1.06t_{w.opt} \end{aligned} \tag{16}$$

where $h_{f.opt}$, b_{opt}, $t_{f.opt}$, and $t_{w.opt}$ are the optimum values of the cross-sectional dimensions of the beam obtained in the first level. Initial values of these variables are randomly chosen between 6% below and 6% above the optimum values at the start of the second level as long as the limits given in Table 2 are not violated. After initiation, penalty values are calculated in the subsequent iterations according to the limits given in Table 2 not according to the limits given in Eq. (16).

For the second level, the finite element model and the optimization algorithm are integrated by developing a code using the built-in ANSYS parametric design language. This code carries out FE analyses and evaluates the results to modify the values of the optimization variables according to the decision criteria of Nelder–Mead algorithm. The same code is also used for the first level, except that analytical equations are used, instead of a FE model, to calculate the objective function.

For the second level, the optimization code initially selects random values for the optimization variables and creates geometries for the die and the preform according to these values. Initial values of the design variables are chosen within the limits given by Eq. (16), while initial values of the processing variables are chosen within the limits given by Table 3. Then, the forging process is simulated by the finite element model using the chosen material properties to obtain the total strain energy, the pressure distribution on the die, and the flash length, L_f. Then, the penalty values and the objective function terms are calculated. Because the number of the optimization variables is 11, 12 initial configurations are randomly generated. In the initial configurations, design and processing constraints are not required to be satisfied except die filling. This is because if die filling is not achieved for the initial configurations, the search algorithm usually converges on a local optimum that does not satisfy this constraint. Having completed 12 FE analyses and obtained the objective function values, the program compares these values according to the decision criteria of Nelder–Mead algorithm, evaluates new values for the optimization variables and creates a new geometry to be analyzed. In each iteration, the worst current configuration is replaced with a better configuration. This procedure is repeated until the stopping criterion is satisfied, which requires the difference between the objective function values of the best and worst configurations to be small, less than 0.005$. In about 250 iterations, convergence is achieved in the second level. As in the first level, the optimization process is repeated at least 20 times, starting from different randomly generated configurations.

3.6. Failure analysis of the I-beam during its use

If the part to be designed and manufactured with the given values for the optimization variables is predicted to fail during its use, a penalty value is added to the objective function in a way that this configuration of the part is to be regarded as unfavorable by the optimization algorithm.

3.6.1. Static failure

If the nominal equivalent stress, σ_{eq}, developed in one region of the part during its use exceeds the yield strength of the material, S_y, static failure is predicted; then a penalty is added to the objective function.

A structural analysis is required to determine the stress state developed due to the loads applied during its use and carry out failure analysis. For this purpose, an analysis based on Bernoulli–Euler beam theory is carried out. The top and the bottom of the beam at the middle section, where the bending moment takes its maximum value with a magnitude of $M_{max} = FL_b/4$, are critical, because the maximum normal stress, σ_{max}, develops in these regions. F is the force applied to the middle of the beam as the worst loading condition during its use. σ_{max} can be calculated using $\sigma_{max} = M_{max}c/I_{zz}$. For an I-beam with the geometry given in Fig. 3, c is equal to $h_f/2$. The analytical formula for the area moment of inertia of the I-beam with respect to the z-axis, I_{zz}, in terms of the cross-sectional dimensions and fillet radii is given in Ref. [63]. Because a pure uniaxial normal stress develops at the top and the bottom, the equivalent stress is equal to σ_{max}.

The intersection between the web and the flange is another critical point, because the normal stress due to bending is combined with shear. The shear stress, τ_i, is calculated by $\tau_i = VQ/I_{zz}t_w$, where V is the shear force, which is equal to $F/2$, t_w is the thickness of the web, and Q is the first moment of area of the region above the intersection between the web and the flange, which is given by $Q = bt_f(h_w + t_f)/2$. The normal stress at the intersection is equal to $\sigma_i = M_{max}(h_w/2)/I_{zz}$.

Thirdly, because the shear force in the beam is mainly supported by the web, it may fail due to shear yielding. The average shear stress in the web of the beam is approximately calculated as

$$\tau_w \approx \frac{V}{h_f t_w} \tag{17}$$

In these three regions, static failure due to yielding is checked by comparing the corresponding equivalent stress with the yield strength of the material.

3.6.2. Lateral buckling

Lateral buckling may occur in thin-walled beams subjected to transverse loads or bending moments when the critical load is exceeded. The lateral buckling is accompanied by the twisting of the beam with respect to the principal axes of inertia. The critical lateral buckling load is calculated [64] as

$$F_{cr} = \frac{4\pi^2}{L_b^2}\sqrt{\frac{3}{\pi^2+6}EI_{yy}\left(GJ + \frac{EC_1\pi^2}{L_b^2}\right)} \tag{18}$$

where E is the elastic modulus, G is the shear modulus, J is the torsion constant, C_1 is the torsion warping constant, which are given by [58]

$$C_1 = \frac{I_{yy}h_w^2}{4} \tag{19}$$

$$J = \frac{2bt_f^3 + (h_w + t_f)t_w^2}{3} \tag{20}$$

The area moment of inertia of the I-beam with respect to the y-axis, I_{yy}, is given in reference [63]. The magnitude of the force applied to the center of the beam, F, (Fig. 1) is compared with F_{cr}. If F is larger than F_{cr}, local buckling is predicted and a penalty is added to the objective function.

3.7. Finite element simulation of the forging process

Owing to the double symmetry in the cross-section of the I-beam, only one quadrant of the workpiece and the die is modeled. Because the workpiece is large in the axial direction and restrained, a two-dimensional model with plane-strain condition is used instead of creating a 3D model. In this way, the computational effort is reduced.

3.7.1. Elements and meshing

Selection of an appropriate element type in the analysis is essential for obtaining reliable results. Selected element should satisfy a set of requirements: Firstly, the element should be suitable for 2D modeling of the structure. Secondly, the element should have large deflection, large strain capabilities because of high deformation of the workpiece during forging. Lastly, a high

order element is more suitable for highly nonlinear deformation process like cold forging. By considering all these requirements, the element type selected in this study is Plane183, which is an 8-node 2D rectangular element. In order to determine the mesh density, a convergence analysis is carried out.

3.7.2. Contact elements

Assuming that the punch does not undergo plastic deformation and its elastic deformations have a negligible effect on the deformation of the workpiece, its surface is defined as non-deformable by using rigid lines surrounding its representative area. The die is defined as rigid target body whereas the workpiece is a deformable contact body. CONTA172 is selected for the deformable lines in the workpiece, and TARGE169 is selected for the non-deformable lines in the punch. The meshed workpiece, contact pairs, and the boundaries before the stroke are depicted in Fig. 5. The major contact is between line L1 and L3–L4.

In this study, the friction coefficient for the interface between the die and the workpiece is taken to be 0.1, which is within the range of values adopted in previous studies [33,38,65].

3.7.3. Boundary conditions

There are only displacement boundary conditions applied on lines and nodes. Symmetry conditions are defined on lines L2 and L5. The punch line is restrained from rotation and movement along the x-axis. It is only allowed to move through a prescribed vertical displacement (stroke), s, in the negative y direction.

3.7.4. Material model

Among the several alternatives to model nonlinear plastic deformation pattern in ANSYS, the selected material model is multi-linear isotropic hardening (MISO) model. MISO is a rate independent model suitable for large strain applications. The flow curve of SAE 1010 [66] is used to define the stress–strain curve.

3.7.5. Yield strength after forging

Because of work hardening of the material during the cold forging process, the yield strength of the undeformed material used in the forging operation, SAE 1010, changes. For this reason, the yield strength of the deformed material should be used in the failure analysis and the design of the part. In this study, the modified yield strength is calculated at the critical locations, where failure is possible, by obtaining the true stress distribution at those locations at the end of the forging process using the finite element model and converting them to engineering stress. The regions around the red lines in Fig. 6 show the locations where failure is possible for an I-beam under a transverse load as discussed in Section 3.6.1.

By simulating the forging process using FEM, equivalent stresses along these lines are obtained; then the averages of these values are calculated. Using the following equation, the true stress values are converted to engineering stress.

$$\sigma_E = \frac{\sigma_T}{e^{\varepsilon_T}} \tag{21}$$

where σ_T is the true stress, ε_T is the true strain, σ_E is the engineering stress, which is used as the yield strength of the material at the corresponding line, if it is larger than the yield strength of the undeformed material. If the maximum stress that develops at a given point during forging does not exceed the yield strength of the material, S_y, one may assume that the yield strength of the material at that point does not change. Accordingly, the yield strength can then be taken as 305 MPa for SAE 1010 after forging. Otherwise, it should be taken as σ_E.

$$S_y = \sigma_E \quad \text{if } \sigma_E > S_y \tag{22}$$

Fig. 7 shows the true equivalent stress distribution in the forged part with typical dimensions at the end of the stroke. The average stress at the top and bottom is obtained to be about 230 MPa. On the other hand, the stress between the flange and the web is 300 MPa, and the stress on the web is 290 MPa as can be seen in Fig. 7. The corresponding engineering stress values are obtained to be 80 MPa, 105 MPa, and 170 MPa respectively. One may conclude that, on the average, there is no significant work hardening of the material during cold forging under typical processing conditions, and thus no change in the yield strength of the material, if a

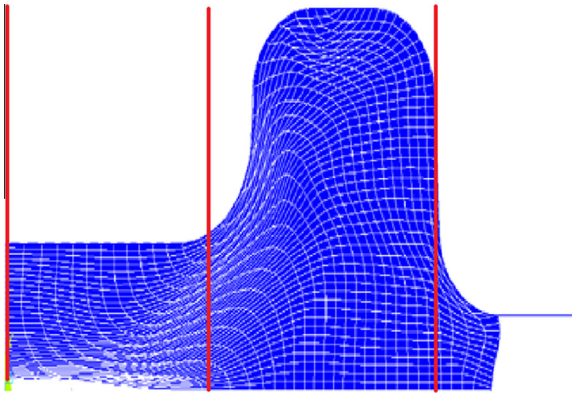

Fig. 6. Expected failure locations in the I-beam.

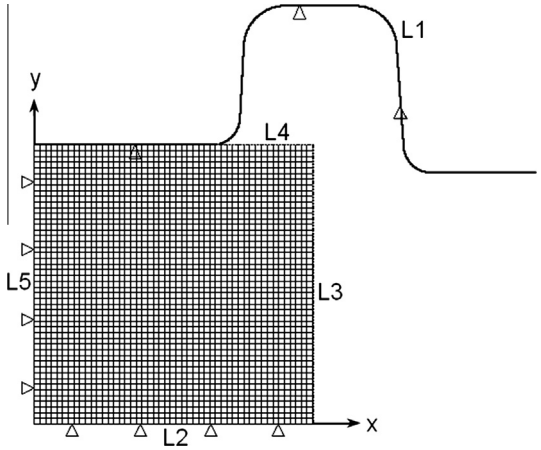

Fig. 5. The FE model with its mesh and the boundary conditions.

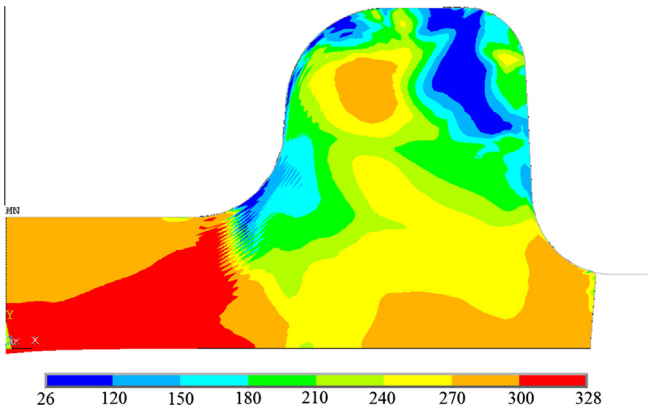

Fig. 7. True equivalent (Von Mises) stress distribution after forging.

Table 4
Results of the first level design optimization in mm for $F = 20$ kN.

h_f	b	t_f	t_w	Cost, $
45.00	35.00	12.31	8.48	2.554

soft material like SAE 1010 is used. However, if a steel harder than SAE 1010 is used like SAE 1040 about 25% increase in yield strength is observed.

4. Results and discussions

By following the aforementioned procedure, concurrent design optimization of an I-beam is achieved using the following values for the constant parameters: The force, F, applied to the center of the I-beam (Fig. 1) is 20 kN. The safety factor is taken as 1.65 due to uncertainties in its magnitude. The length of the beam is 400 mm. The price of the material (SAE 1010), p_{mat}, is taken as 0.79 $/kg, while the price of electricity is taken as 0.113 $/kW h. The cost of machining the surface obtained after the shearing operation is 40 $/m^2. The elastic modulus, E, of the material is 207 GPa, its shear modulus, G, is 79.3 GPa, and its density, ρ, is 7870 kg/m^3. In the first level of the optimization, the material cost of the I-beam is minimized using the cross-section dimensions as variables, the height, h_f, and the width, b, of the beam, the thickness of the flange, t_f, and the thickness of the web, t_w. Only the design constraints are considered to avoid buckling and static yielding failures during the use of the part. After repeated runs starting from initial random configurations, the results presented in Table 4 are obtained for the first level. The optimum height, h_f, and the optimum width, b, are equal to the upper limits of these dimensions. This is understandable because if these dimensions are increased while keeping the volume constant, the moment of area, I_{zz}, will increase, thus the load bearing capacity of the beam will increase as long as the web and the flange are not too thin to cause local buckling. The algorithm reduces the flange thickness, t_f, and the web thickness, t_w until the stresses at the top or bottom and at the intersection between the web and the flange become critical. On the other hand, the average shear stress in the flange given by Eq. (17) is not critical. Besides, local bucking failure mode does not become active in all runs; this is because the flange and web thicknesses are large.

In the second level, seven manufacturing parameters and four design parameter are used as optimization variables to minimize the total cost including material cost, forging cost, shearing cost, and machining cost. Initial designs are randomly generated around the neighborhood of the optimal values (Table 4) obtained in the first level. According to Eq. (16), the upper and lower limits within which random numbers are generated are $42.3 \leqslant h_{f.ini} \leqslant 45$, $32.9 \leqslant b_{ini} \leqslant 35$, $11.57 \leqslant t_{f.ini} \leqslant 13.05$, and $7.97 \leqslant t_{w.ini} \leqslant 8.99$ in mm. After randomly obtaining the initial designs, the constraint limits given in Table 2 are applied. As for the processing variables, their initial values are randomly chosen within their constraint limits given in Table 3. The optimization process is repeated at least 20 times. The best solution is presented in Table 5.

Small changes occur in the values of the design variables (h_f, b, t_f, t_w) in the second level as expected, because local search is done around the optimum values obtained in the first level. None of the constraints on the optimization variables given in Tables 2 and 3 are active; optimal values of the design variables are not close to the constraint limits except the height, h_f, and the width, b, of the beam. The total cost is calculated as 3.126 $, while the material cost is 2.796 $, the forging cost is 0.224 $, the shearing cost is 0.010 $, and the machining cost is 0.097 $. The material cost is about 90% of the total cost. Even though depreciation of machinery is taken into account, the material cost comprises a significant portion of the total cost. This is understandable, because the material cost includes all the costs involving extraction of the metal from mines, transportation, obtaining the raw material with the given composition, etc. Forging, shearing, and machining are only the last operations. The difference in the material costs obtained in the first and second levels arises because in the second level optimization, the material of the flash cut off after forging is also included. The maximum contact pressure is 1078 MPa. This means it is almost at its limit, 1080 MPa, which is 10% lower than the allowable contact pressure on the die (1200 MPa). Buckling is not critical. This is because the resulting shape cannot be considered as a thin-walled structure. Only the static failure condition at the top or bottom is critical, where the maximum equivalent stress reaches its allowable value, while static failure at the web or web-flange interface is not critical. The constraint on the flash length is not active; it is 1.71 mm; its lower and upper limits are 0.0 mm and 2.0 mm. Fig. 8 shows the shape of one quadrant of the optimized I-beam and the true equivalent stress distribution. Largest deformation occurs in the web; for this reason, stresses are also large in that region.

Tables 6 and 7 present the results of the first and second level optimizations, respectively, for the case in which the force applied to the middle of the beam during its use is 5% higher, that means $F = 21$ kN. When the force is increased, the algorithm tries to increase the flange thickness, t_f, which effectively increases the

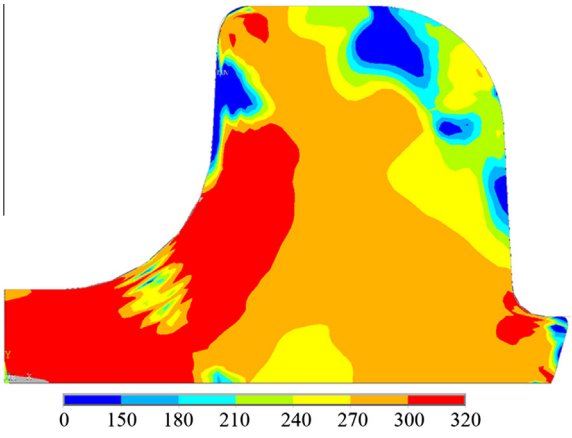

Fig. 8. True equivalent (Von Mises) Stress distribution in one quadrant of the optimized I-beam after forging.

Table 6
Results of the first level design optimization in mm for high load, $F = 21$ kN.

h_f	b	t_f	t_w	Cost, $
45.00	35.00	15.30	8.56	2.950

Table 5
Results of the second level concurrent optimization in mm for $F = 20$ kN.

h_f	b	t_f	t_w	r_1	r_2	r_3	r_4	t_b	H	ℓ	Cost $
44.77	34.35	12.68	8.51	6.98	1.38	5.85	1.48	3.03	21.95	0.55	3.126

Table 7
Results of the second level concurrent optimization in mm for high load, $F = 21$ kN.

h_f	b	t_f	t_w	r_1	r_2	r_3	r_4	t_b	H	ℓ	Cost $
44.96	34.84	14.91	8.51	6.82	1.70	3.81	6.92	0.51	22.79	0.02	3.337

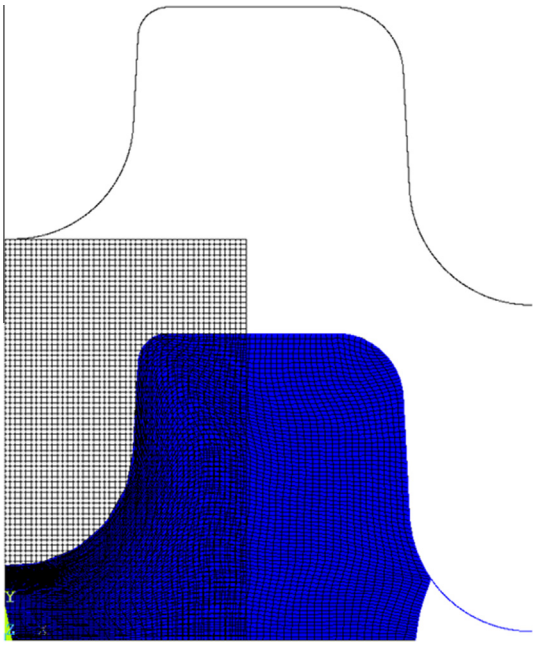

Fig. 9. Initial shape of one quadrant of the preform and the final forged part.

Table 8
Results of the first level design optimization in mm for low load, $F = 18$ kN.

h_f	b	t_f	t_w	Cost, $
45.00	35.00	9.03	8.65	2.132

moment of inertia of the cross-section, I_{zz}, in order to reduce the bending stress, $\sigma_{max} = M_{max}c/I_{zz}$. On the other hand, the web thickness, t_w, is slightly increased to overcome bending stresses and shear stresses. Fig. 9 shows the initial shape of one quadrant of the preform and the final forged part. The material completely fills the die as required.

Tables 8 and 9 present the results of the concurrent optimization for the case in which the force is 10% lower, i.e. F is 18 kN. If a lower force is applied, the algorithm reduces the thickness of the flange, t_f, to reduce the material use. The width, b, and the height, h_f, of the cross-section are again at their limits as in the other cases. One may conclude that the most effective parameter is the flange thickness, t_f, after h_f and b.

In Table 10, the second level concurrent optimization results are presented for the case in which not only the cut region but also the rest of the top and bottom surfaces of the beam are machined. The cut region has a rougher surface; for this reason the machining cost is higher ($p_{fm} = 80\$/m^2$), while the rest of the surface is smoother forged surface and it machined with the price of $p_m = 40\$/m^2$. Because the same force is applied during its use ($F = 20$ kN), the same results of the first level optimization given in Table 4 are used in the second level. For the optimum configuration, the material cost is 2.794$, the forging cost is 0.206$, the shearing cost is 0.013$, and the machining cost is 1.329$. Even though the machining cost becomes a significant portion of the total cost, it is still less than half of the material cost, for this reason similar results are obtained as in the case of small machining surface (Table 5). One may conjecture that if the machining cost were larger than the material cost, the algorithm would try to reduce the width, b, i.e. the top and bottom surface area.

5. Conclusions

Design parameters not only affect the performance of a product, but also the feasibility, effectiveness, and efficiency of manufacturing. Processing parameters, in turn, affect the performance of the part. Therefore, effective optimization of a product requires a joint consideration of design and manufacturing aspects. In this study, a concurrent design optimization methodology is developed to minimize the total cost of cold-forged parts using both design and manufacturing parameters as optimization variables. The method is applied to the design and forging of an I-beam under a centric load and its total cost is minimized including the material cost, the forging cost, and the post manufacturing shearing and machining costs. The design variables are the cross-sectional dimensions of the I-beam; the manufacturing variables are the fillet radii, thickness of the flash, and the preform dimensions. In the optimizations, both design and manufacturing constraints are applied. The design constraints include failure conditions due to static yielding and local buckling during the use of the beam and the manufacturing constraints include die filling, the maximum allowable pressure on the die, and limited flash out of the die.

Considering the difficulty of optimizing the part design and the processing design at the same time, a multilevel optimization approach is adopted. In the first level, the design of the product is optimized; in the second level, both the product design and the forging process are optimized. Nelder–Mead, which is a zero-order algorithm, is selected as the search algorithm to find the optimum values for the process and product design parameters.

Table 9
Results of the second level concurrent optimization in mm for low load, $F = 18$ kN.

h_f	b	t_f	t_w	r_1	r_2	r_3	r_4	t_b	H	ℓ	Cost $
44.74	34.19	8.91	8.42	9.24	1.70	3.81	6.92	0.51	22.79	0.02	2.648

Table 10
Results of the second level optimization in mm with larger machined surface.

h_f	b	t_f	t_w	r_1	r_2	r_3	r_4	t_b	H	ℓ	Cost $
44.84	34.37	12.86	8.90	5.85	2.14	3.03	1.83	3.57	21.38	0.14	5.294

Because, it is a deterministic local search algorithm, the optimization process is repeated at least 20 times starting from randomly chosen configurations within the feasible domain in order to obtain the global optimum configuration or a near global optimum. Analysis of the cold forging process is performed and the optimization process is conducted using ANSYS.

In a multilevel approach, the optimization variables to be used at different levels should be chosen carefully. In the first level, the design variables should be used to obtain the optimum part design satisfying the design constraints. Because in the first level, the manufacturing constraints are not used, manufacturability of the part is not ensured. In the second level, not only the manufacturing parameters but also all of the design parameters that influence the effectiveness of manufacturing should be used as optimization variables. In this way, if the design found in the first level turns out to be not appropriate in terms of manufacturability, the design can be changed in the second level. While the globally optimal values of the design variables are searched in the first level within a large solution domain, design optimization is performed in the second level within the close neighborhood of the optimal values obtained in the first level. After the second level optimization is performed, optimum product and process designs are obtained.

The proposed concurrent design optimization method proved to be effective. It not only ensured the manufacturability of the designed part, but also optimized the part design as well as the process design. The method developed in this study can be applied to the optimization of different forged products. For different parts, different variables and constraints need to be defined and a reliable FE model of the process needs to be developed.

Acknowledgment

This paper is based on the work supported by the Scientific Research Projects of Bogazici University with the code number 08A602.

References

[1] Altan T, Ngaile G, Shen G. Cold and hot forging, fundamentals and applications. OH: ASM International; 2005.
[2] Poursina M, Parvizian J, Antonio CAC. Optimum pre-form dies in two-stage forging. J Mater Process Technol 2006;174(1–3):325–33.
[3] Lu B, Ou H, Long H. Die shape optimisation for net-shape accuracy in metal forming using direct search and localised response surface methods. Struct Multidisc Optimiz 2011;44(4):529–45.
[4] António CC, Castro CF, Sousa LC. Optimization of metal forming processes. Comp Struct 2004;82(17–19):1425–33.
[5] Fourment L, Balan T, Chenot JL. Optimal design for non-steady-state metal forming processes – I. Shape optimization method. Int J Numer Meth Eng 1996;39:51–65.
[6] Fourment L, Chenot JL. Optimal design for non-steady-state metal forming processes – II. Application of shape optimization in forging. Int J Numer Meth Eng 1996;39:33–50.
[7] Zhao G, Wright E, Grandhi RV. Preform die shape design in metal forming using an optimization method. Int J Numer Meth Eng 1997;40(7):1213–30.
[8] Castro CF, Sousa CL, António CAC, César de Sá JMA. An efficient algorithm to estimate optimal preform die shape parameters in forging. Eng Comput 2001;18(7–8):1057–77.
[9] Srikanth A, Zabaras N. Shape optimization and preform design in metal forming processes. Comp Meth Appl Mech Eng 2000;190(13–14):1859–901.
[10] Shim H. Optimal preform design for the free forging of 3D shapes by the sensitivity method. J Mater Process Technol 2003;134(1):99–107.
[11] Valente RAF, Andrade-Campos A, Carvalho JF, Cruz PS. Parameter identification and shape optimization: an integrated methodology in metal forming and structural applications. Optimiz Eng 2011;12(1–2):129–52.
[12] António CAC, Dourado NM. Metal-forming process optimization by inverse evolutionary search. J Mater Process Technol 2002;121(2–3):403–13.
[13] Kang Z, Luo Y. Sensitivity analysis of viscoplastic deformation process with application to metal preform design optimization. Eng Optimiz 2012;44(12):1511–23.
[14] Castro CF, António CAC, Sousa LC. Optimisation of shape and process parameters in metal forging using genetic algorithms. J Mater Process Technol 2004;146(3):356–64.
[15] Poursina M, Antonio CAC, Castro CF, Parvizian J, Sousa LC. Preform optimal design in metal forging using genetic algorithms. Eng Comput 2004;21:631–50.
[16] António CAC, Castro CF, Sousa LC. Eliminating forging defects using genetic algorithms. Mater Manufact Process 2005;20:509–22.
[17] Chung JS, Hwang SM. Process optimal design in forging by genetic algorithm. J Manufact Sci Eng, Trans ASME 2002;124(2):397–408.
[18] Biglari FR, O'Dowd NP, Fenner RT. Optimum design of forging dies using the finite element method. In: 5th ACME-UK conference. London: Imperial College; 1997. p. 100–4.
[19] Repalle J, Grandhi RV. Reliability-based preform shape design in forging. Commun Numer Meth Eng 2005;21(11):607–17.
[20] Khoury I, Giraud-Moreau L, Lafon P, Labergére C. Towards an optimisation of forging processes using geometric parameters. J Mater Process Technol 2006;177(1–3):224–7.
[21] Gao Z, Grandhi RV. Microstructure optimization in design of forging processes. Int J Mach Tools Manufact 2000;40(5):691–711.
[22] Repalle J, Grandhi RV. Design of forging process variables under uncertainties. J Mater Eng Perform 2005;14(1):123–31.
[23] Zhao GQ, Huff R, Hutter A, Grandhi RV. Sensitivity analysis based preform die shape design using the finite element method. J Mater Eng Perform 1997;6:303–10.
[24] Zhao X, Zhao G, Wang G, Wang T. Preform die shape design for uniformity of deformation in forging based on preform sensitivity analysis. J Mater Process Technol 2002;128:25–32.
[25] Zhao G, Ma X, Zhao X, Grandhi RV. Studies on optimization of metal forming processes using sensitivity analysis methods. J Mater Process Technol 2004;147(2):217–28.
[26] Zhao G, Wright E, Grandhi RV. Sensitivity analysis based preform die shape design for net-shape forging. Int J Mach Tools Manufact 1997;37(9):1251–71.
[27] Kim DJ, Kim BM, Choi JC. Determination of the initial billet geometry for a forged product using neural networks. J Mater Process Technol 1997;72:86–93.
[28] Ou H, Lan J, Armstrong CG, Price MA. An FE simulation and optimisation approach for the forging of aeroengine components. J Mater Process Technol 2004;151(1–3):208–16.
[29] Lu B, Ou H, Armstrong CG, Rennie A. 3D die shape optimisation for net-shape forging of aerofoil blades. Mater Des 2009;30(7):2490–500.
[30] Lu B, Ou H. Stochastic finite–element modelling and optimization for net-shape forging of three-dimensional aero-engine blades. Proc Inst Mech Eng 2011;225:71–85.
[31] Lu B, Ou H, Cui S. Shape optimization of preform design for precision close-die forging. Struct Multidisc Optimiz 2011;44:785–96.
[32] Ou H, Wang P, Lu B, Long H. Finite element modelling and optimisation of net-shape metal forming processes with uncertainties. Comp Struct 2012;90–91(1):13–27.
[33] Tumer H, Sonmez FO. Optimum shape design of die and preform for improved hardness distribution in cold forged parts. J Mater Process Technol 2009;209(3):1538–49.
[34] Cheng H, Grandhi RV, Malas JC. Design of optimal process parameters for non-isothermal forging. Int J Numer Meth Eng 1994;37(1):155–77.
[35] Yang C, Ngaile G. Preform design for forging and extrusion processes based on geometrical resemblance. Proc Inst Mech Eng, Part B: J Eng Manufact 2010;224(9):1409–23.
[36] Jolgaf M, Hamouda AMS, Sulaiman S, Hamdan MM. Development of a CAD/CAM system for the closed-die forging process. J Mater Process Technol 2003;138(1–3):436–42.
[37] Meng F, Labergere C, Lafon P, Duguy M, Daniel L. Multi-objective optimization based on meta-models of an aeronautical hub including the ductile damage constraint. Int J Damage Mech 2014;23(8):1055–76.
[38] Roy S, Ghosh S, Shivpuri R. A new approach to optimal design of multi-stage metal forming processes with micro genetic algorithms. Int J Mach Tools Manufact 1997;37(1):29–44.
[39] Kim DH, Kim DJ, Kim BM. Application of neural networks and statistical methods to process design in metal forming processes. Int J Adv Manufact Technol 1999;15(12):886–94.
[40] Duggirala R, Shivpuri R, Kini S, Ghosh S, Roy S. Computer aided approach for design and optimization of cold forging sequences for automotive parts. J Mater Process Technol 1994;46:185–98.
[41] Yanhui Y, Dong L, Ziyan H, Zijian L. Optimization of preform shapes by RSM and FEM to improve deformation homogeneity in aerospace forgings. Chin J Aeronaut 2010;23:260–7.
[42] Okada M, Kitayama S, Kawamoto K, Chikahisa J, Yoneyama T. Determination of back-pressure profile for forward extrusion using sequential approximate optimization. Struct Multidisc Optimiz 2015;51(1):225–37.
[43] Meng F, Labergere C, Lafon P. Methodology of the shape optimization of forging dies. Int J Mater Form 2010;3:927–30.
[44] Chenot J, Massoni E, Fourment L. Inverse problems in finite element simulation of metal forming processes. Eng Comput 1996;13(2–4):190–225.
[45] Vieilledent D, Fourment L. Shape optimization of axisymmetric preform tools in forging using a direct differentiation method. Int J Numer Meth Eng 2001;52(11):1301–21.
[46] Thiyagarajan N, Grandhi RV. Multi-level design process for 3-D preform shape optimization in metal forming. J Mater Process Technol 2005;170(1–2):421–9.
[47] Khaleed HMT, Samad Z, Othman AR, Mujeebu MA, Abdullah AB, Ahmed NJS, et al. Flash-less cold forging and temperature distribution in forged

autonomous underwater vehicle hubs using FEM analysis and experimental validation. Int J Mech Mater Eng 2011;6(2):291–9.
[48] Thiyagarajan N, Grandhi RV. 3D preform shape optimization in forging using reduced basis techniques. Eng Optimiz 2005;37(8):797–811.
[49] Bonte MHA, Fourment L, Do T, Boogaard AH, Huetink J. Optimization of forging processes using finite element simulations: a comparison of sequential approximate optimization and other algorithms. Struct Multidisc Optimiz 2010;42(5):797–810.
[50] Li X-B, Zhang Z-M, Wang Q, Yang Y-B, Li G-J. Forming process optimization for non-axisymmetrical complex component based on FEM simulation and experiment. J Adv Manufact Technol 2014;72(9–12):1717–25.
[51] Esche SK, Chassapis C, Manoochehri S. Concurrent product and process design in hot forging. Concurr Eng: Res Appl 2001;9(1):48–54.
[52] Janakiraman V, Saravanan R. Concurrent optimization of machining process parameters and tolerance allocation. Int J Adv Manufact Technol 2010;51(1–4):357–69.
[53] Chang K, Bryant IH. Concurrent design and manufacturing of aircraft torque tubes. J Mater Process Technol 2004;150:151–62.
[54] Al-Ansary MD, Deiab IM. Concurrent optimization of design and machining tolerances using the genetic algorithms method. Int J Mach Tools Manufact 1997;37(12):1721–31.
[55] Chen L, Simon L. A computerized team approach for concurrent product and process design optimization. CAD Comp Aided Des 2002;34:57–69.
[56] Ozturk M. Optimization of forging processes with a concurrent approach, Master Thesis. Bogazici University; 2009.
[57] Ozturk M, Sonmez FO. Optimization of forging processes with a concurrent approach. In: 5th International conference on design and production of machines and dies/mold; 2009.
[58] Andrade A, Camotim D, Providência e Costa P. On the evaluation of elastic critical moments in doubly and singly symmetric I-section cantilevers. J Construct Steel Res 2007;63(7):894–908.
[59] Schey JA. Introduction to manufacturing processes. 3rd ed/. Boston: McGraw-Hill Book Company; 1999.
[60] Akbulut M, Sonmez FO. Design optimization of laminated composites using a new variant of simulated annealing. Comp Struct 2011;89:1712–24.
[61] Mathews JH. Numerical methods using matlab. 3rd ed. Prentice Hall; 1999.
[62] Gürdal Z, Haftka RT, Hajela P. Design and optimization of laminated composite materials. John Wiley & Sons; 1999.
[63] Kocaoglan S. Concurrent design and process optimization in forging, Master Thesis. Bogazici University; 2013.
[64] Yoo CH, Lee S. Stability of structures: principles and applications. Butterworth-Heinemann; 2011.
[65] Petruška J, Janíček L. On the evaluation of strain inhomogeneity by hardness measurement of formed products. J Mater Process Technol 2003;143–144(1):300–5.
[66] Boller C, Seeger T. Materials data for cyclic loading part A: unalloyed steels. Amsterdam; New York: Elsevier; 1987.